



Titanium dioxide nanotubes conjugated with quercetin function as an effective anticancer agent by inducing apoptosis in melanoma cells

Surendra Gulla¹ · Dakshayani Lomada² · Prasanna Babu Araveti³ · Anand Srivastava³ · Mamatha Kumari Murikinati⁴ · Kakarla Raghava Reddy⁵ · Inamuddin⁶ · Madhava C. Reddy¹ · Tariq Altalhi⁷

Received: 21 November 2020 / Accepted: 18 March 2021 / Published online: 26 April 2021

© Islamic Azad University 2021

Abstract

Cancer is a leading cause of death throughout the world. Melanoma is a skin cancer with a significant impact on global public health. Application of nanotechnology in the field of cancer diagnosis, drug delivery, imaging and therapy, has the most attractive approach as nanoparticles reach target sites easily due to their unique properties. Previous studies have shown that titanium dioxide nanotubes (TNT) and quercetin are effective anticancer agents. However, conjugated TNT with quercetin (TNT–Qu) as a combinational treatment is unexplored yet. This study is aimed to explore the anticancer activity of TNT, quercetin, and TNT–Qu in B16F10 melanoma skin cancer cells. TNT–Qu significantly inhibited proliferation at 25 µg/mL of IC 50 lower than quercetin (34 µg/mL) and TNT alone (72 µg/mL). TNT–Qu treatment inhibited migration and significantly induced 60.29% apoptosis in melanoma cells when compared to TNT (14.14%) or quercetin (44.86%) alone treatment. Furthermore, quercetin and TNT–Qu decreased the reactive oxygen species and superoxide levels due to quercetin's antioxidant properties. TNT–Qu treatment arrested 55.5% cells in G2/M phase more than quercetin (30.7%) or pristine TNT (3.7%) treatment. The molecular mechanism of TNT–Qu on melanoma cells revealed that it enhanced the cleaved caspase-3 levels and induced more apoptosis than TNT or quercetin alone. Hence, Novel TNT–Qu exhibited enhanced anticancer properties and could be a potential therapeutic combinational molecule for the treatment of skin cancer.

✉ Inamuddin
inamuddin@zhcet.ac.in

✉ Madhava C. Reddy
cmadhavareddy@gmail.com

¹ Department of Biotechnology and Bioinformatics, Yogi Vemana University, Kadapa, AP 516005, India

² Department of Genetics and Genomics, Yogi Vemana University, Kadapa, AP 516005, India

³ National Institute of Animal Biotechnology, Hyderabad, TS 500032, India

⁴ Department of Materials Science and Nanotechnology, Yogi Vemana University, Kadapa, AP 516005, India

⁵ School of Chemical and Biomolecular Engineering, The University of Sydney, Sydney, NSW 2006, Australia

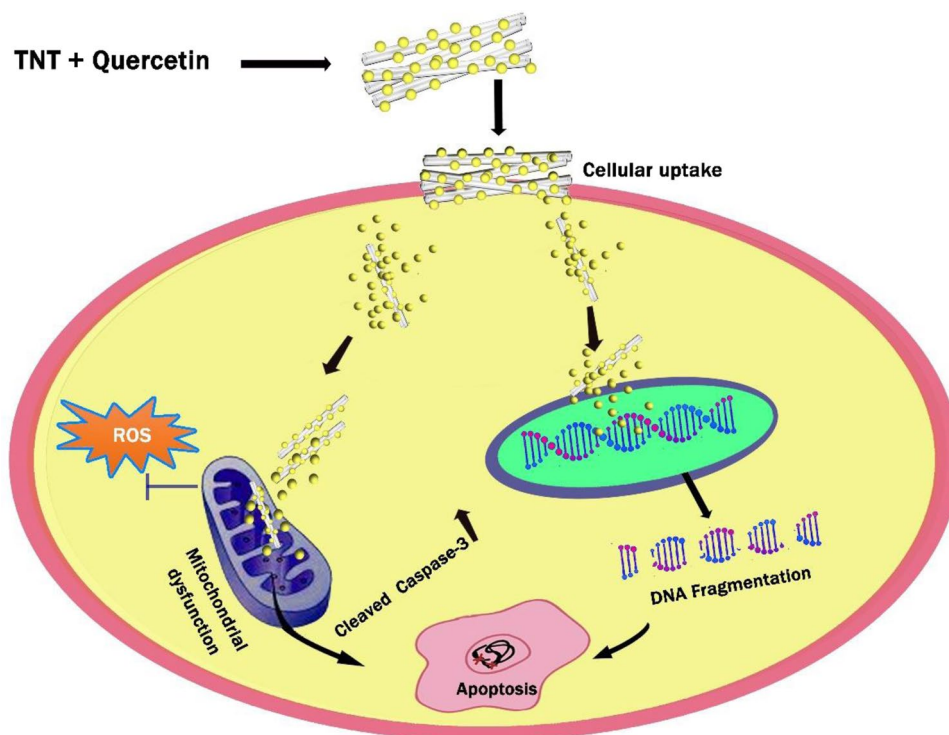
⁶ Advanced Functional Materials Laboratory, Department of Applied Chemistry, Zakir Husain College of Engineering and Technology, Faculty of Engineering and Technology, Aligarh Muslim University, Aligarh 202 002, India

⁷ Department of Chemistry, College of Science, Taif University, P.O. Box 11099, Taif 21944, Saudi Arabia



Graphic abstract

Schematic representation of the proposed mechanism of TNT, quercetin and TNT–Qu inducing apoptosis in B16F10 melanoma cells. TNT–Qu enhanced the cleaved caspase-3 and induced caspase-dependent apoptosis. Importantly, it down-regulates the ROS and dysfunctions mitochondria and enhances the DNA fragmentation.



Keywords Titanium dioxide nanotubes · B16F10 melanoma cells · Quercetin · Apoptosis · Caspase-3

Introduction

Cancer is a very complex disease and second leading cause of death globally. Melanoma is the most common type of skin cancer and is originated in skin cells called melanocytes [1]. These melanocytes produce melanin and give color to the skin [2]. In melanoma, tumors appear in black or brown color due to enhanced expression of melanin. The primary cause of this cancer is UV radiation which damages the ability of skin cell proliferation, DNA repair [3], immune surveillance, and apoptosis. Failure of these pathways leads to the inactivation of the tumor suppressor genes or activation of oncogenes and, thus, allows skin tumor development [4]. There are four main types of melanoma. First, superficial spreading melanoma is the most common and dominant type, observed in about 70% of cancer cases. Second and third nodular melanoma and Lentigo maligna melanoma, which are detected in about 15–20% and of the 10–15%, of the cancer cases. All these three types of cancer occur on the top layers of the skin. Finally, Acral lentiginous melanoma is the most common in people with dark skin which spreads

superficially and it is about 5% of the cancer cases [5, 6]. According to the AIM at melanoma foundation, 132,000 new cases are identified every year worldwide. In 2018, it was estimated that 91,270 new cases are registered and 9320 deaths from the disease were reported in United States and it is the least common but very dangerous skin cancer in the world. Clinical data demonstrated that functionalized nanoparticles enhance tumor reduction and reduce side effects [7–9].

TiO₂ nanoparticles have unique properties and can be utilized in food, textiles, photo-remediation catalysts, drug delivery, solar cells, etc. [10]. Our previous data showed that TiO₂ reduced the levels of pro-inflammatory cytokine HMGB1 and inhibited breast cancer cell proliferation, blood vessel formation, and regulated tumor suppressor genes such as MDA7 and p53 [11, 12]. Furthermore, the immunomodulatory properties of TiO₂ were described [12]. Currently, commonly used cancer therapies mainly include surgery, radiation, and chemotherapy. However, these methods are at the risk of damaging the adjacent normal tissue. Nanoparticles conjugated with chemotherapeutic agents overcome this limitation by precise



targeting of the tumor cells, and have reduced side effects [13, 14]. The Food and Drug Administration (FDA) approved few nanoparticle-based products like PEGylated liposomal doxorubicin, liposomal doxorubicin, liposomal daunorubicin, and nanoparticle albumin (NAB) paclitaxel for breast, ovary, lung, pancreas, and Kaposi's sarcoma treatment [15].

Metallic nanoparticles have different physical, chemical, and optical properties. By modifying chemical, surface area, and charge, the nanoparticles' size achieves the targets in tumor sites [16]. Hence, nanoscale particles are the frontier of nanotechnology with their application as a biomaterial. Although TNT alone exhibits anticancer activity, this study investigates the enhancement in anticancer activity of TNTs by conjugating it with quercetin. To our knowledge, there is no information on the role of TNT alone or the combination of TNT with quercetin, especially on melanoma cells. Quercetin is a phenolic flavonoid, and it is found in green leafy vegetables and fruits. Quercetin is known to have anticancer, antioxidant, and antiviral properties. Quercetin inhibited the proliferation of different cancer cell lines like breast, colorectal, lung, ovarian, melanoma, glioblastoma and leukemia [17–20]. Although previous data showed that quercetin inhibited the proliferation of melanoma cancer cells B16F10 in vitro, the complete mechanism of quercetin on B16F10 melanoma cells was not known and the impact of TNT and TNT with quercetin as combinational therapy is unexplored yet [21]. Although earlier reports showed that titanate particles and quercetin individually exhibited anticancer activity, this is the first report on potential anticancer activity of TNT–Qu on B16F10 melanoma cells.

The present work reports the synthesis of TNT conjugated with quercetin and characterized using various physicochemical techniques for its functional groups. The study demonstrates the beneficial effect of TNT–Qu on in vitro anticancer activity against B16F10 melanoma cells. Furthermore, we were able to show the possible mechanism of action for its anticancer activity by MTT assay, and cell migration was studied by scratch assay. Apoptosis, DNA fragments, and ROS (reactive oxygen species) levels were evaluated by flow cytometry. Immunoblotting was used to study the expression levels of cleaved caspase-3, an apoptotic protein. Our results revealed that TNT–Qu was cytotoxic to B16F10 by inducing apoptosis and arresting cell cycle and also activating apoptotic protein cleaved caspase-3 when compared to quercetin or TNT alone.

Materials and methods

Chemicals

TiO₂, quercetin, 4,6 diamidino 2 phenylindole (DAPI) are purchased from Sigma Aldrich(USA). Dulbecco Modified

Eagle's Medium (DMEM), fetal bovine serum (FBS), antibiotic solution (ABS), trypan blue, phosphate buffered saline (PBS-pH-7.4), 3-(4,5-dimethylthiazol-2-yl)-2,5-diphenyl tetrazolium bromide (MTT) were purchased from HiMedia Laboratories (India). Cleaved caspase-3, Annexin V–FITC and Apo direct kit from BD Biosciences (USA). ROS/Superoxide detection kit bought from Abcam (UK). Signal fire ECL reagent and actin antibodies were purchased from cell signaling (USA). Anti-rabbit mouse secondary antibodies conjugated with HRP were purchased from Bio-Rad (USA).

Preparation of stock solutions

10 mg/mL of TNT and TNT–Qu (10 mg/mL) was dispersed in 1 mL dimethyl sulfoxide (DMSO) and ultrasonicated for 15 min, stored at 4 °C. 10 mg/mL quercetin was dissolved in DMSO.

Cells and cell culture

B16F10 melanoma cells were obtained from the national centre for Cell Sciences (Pune, India). Cells were grown in culture flask containing DMEM supplanted with 10% FBS, 1% antibiotic solution, and incubated at 37 °C with 5% CO₂ in a humidified atmosphere.

Synthesis of TiO₂ nanotubes (TNT)

Synthesis of TNTs was performed according to Kumar et al. [22]. Briefly, 2.5 g of TiO₂ was dispersed in 10 M NaOH, which was then transferred to autoclave for hydrothermal treatment at 180 °C for 20 h. Obtained white slurry was washed with distilled water. Further, it is treated with HCl and ethanol and dried at 80 °C for 16 h.

Conjugation of TNT nanotubes with quercetin

For conjugation of nanotubes with quercetin, 0.1 mg/mL quercetin was dissolved in acetone and 1 mg/mL TNT was dispersed in PBS pH-7.4 and sonicated for 15 min at ambient temperature. Then, dissolved quercetin was added to the sonicated TNT and stirred continuously for 45 min. The resultant mixture was purified by ultracentrifugation using Beckman optima XPN100 for 40 min at 15 °C. The excess amount was washed with PBS-pH-7.4 and the sample dried at 60 °C for 12 h. The resulted TNT conjugate quercetin was used for further characterization [23].

Characterization methods

Physicochemical techniques were used to characterize TNT, quercetin, and TNT–Qu. The structure and morphology of



TNT and TNT–Qu were analyzed using HR-TEM (JEOL–Japan). The crystalline nature of the compounds was characterized using X-ray diffraction (XRD) method using (Rigaku Miniflex) with Cu K α radiation at 2 θ angles varying from 20° to 80°. DRS UV (Shimadzu-1800) spectra were performed for studying the absorption spectra of TNT, quercetin, and TNT–Qu. Fourier Transformation of Infrared Spectroscopy was used to identify functional groups in TNT, quercetin, and TNT–Qu with a Perkin Elmer spectrum RX I Fourier IR transformation system, in the frequency range of 500–4000 cm $^{-1}$ and a resolution of 4 cm $^{-1}$.

TNT, quercetin and TNT–Qu anticancer activity

MTT protocol

The cytotoxic property of TNT, quercetin and TNT–Qu was studied using MTT assay. B16F10 cells at 1×10^4 /well were treated with concentrations ranging from 1 to 100 $\mu\text{g}/\text{mL}$ of TNT, TNT–Qu or quercetin which were incubated in 5% CO $_2$ incubator for 24 h. Cytotoxicity was measured by following the MTT cell assay kit protocol (HiMedia laboratories, India). After completion of the incubation time, 20 μL of 5 mg/mL MTT solution was added to the wells and incubated in a CO $_2$ incubator for 4 h at 37 °C. MTT crystals were solubilized by adding 100 μL of solubilizing buffer to each well and recorded the absorbance at 570 nm in ELISA reader with a 650 nm reference filter. Viability was calculated using the formula

$$\% \text{ of viability} = \frac{\text{OD of test sample} - \text{OD of blank}}{\text{OD of control}} \times 100.$$

Scratch assay

Scratch assay is used for studying the migration of the cells. Using this model, we investigated TNT, quercetin, and TNT–Qu's effect on the migration of B16F10 melanoma cells at 0 and 24 h. The protocol followed briefly was 1×10^6 per well B16F10 cells were seeded in 6-well plates. The scratch was created with the help of 200 μL tip and floated cells were removed. Then, the cells were exposed with 40 $\mu\text{g}/\text{mL}$ of TNT or 25 $\mu\text{g}/\text{mL}$ of quercetin, or 25 $\mu\text{g}/\text{mL}$ of TNT–Qu for 24 h. Images were captured using an inverted microscope at 5 \times magnification and compared scratch length on 0 and 24 h with the help of image j software.

Apoptosis assay

Annexin-V assay was carried out according to BD Biosciences procedure protocol. Briefly, 0.5×10^6 B16F10 cells per well were cultured in six-well plates and allowed to adhere

overnight. Cells were treated with TNT, quercetin or TNT–Qu (40, 25, 25 $\mu\text{g}/\text{mL}$), respectively, for 24 h. After completion of treatment, cells were harvested and incubated in a cold binding buffer. 5 μL of Annexin V conjugated to FITC and 5 μL of propidium iodide were added and incubated in dark condition for 15 min at room temperature. Flow cytometry (BD LSR-Fortessa, BD Biosciences) was immediately conducted and data were analyzed using flow Jo software.

Reactive oxygen species and superoxides

Cellular ROS/Superoxide kit (Abcam) was used to study ROS/Superoxides. Briefly, 0.5×10^6 cells were incubated per well in six-well plates and added 40 $\mu\text{g}/\text{mL}$ of TNT, 25 $\mu\text{g}/\text{mL}$ of quercetin or 25 $\mu\text{g}/\text{mL}$ of TNT–Qu for 24 h, *N*-acetyl-L cysteine used as a negative control and 100 μM pyocyanin as a positive control. Cells were harvested from each group and incubated with the ROS superoxide mix in normal tissue culture conditions for 30 min and analyzed on flow cytometry.

Cell cycle regulation

Cell cycle regulation was analyzed using DAPI. Briefly, 0.5×10^6 cells per well were seeded on six-well plate and treated with 40 $\mu\text{g}/\text{mL}$ of TNT, 25 $\mu\text{g}/\text{mL}$ of quercetin or 25 $\mu\text{g}/\text{mL}$ of TNT–Qu. Cells were harvested and washed with PBS. Then, cells were fixed in 70% cold ethanol and placed overnight at –20 °C. Ethanol was removed from the cells and incubated with DAPI at 1 mg/mL concentration in dark conditions for 10 min and analyzed on flow cytometry (BD LSR-Fortessa, BD Biosciences).

DNA fragmentation analysis

DNA fragments were studied with the help of Apo-Direct kit obtained from BD Biosciences. After treatment of cells with 40 $\mu\text{g}/\text{mL}$ of TNT, 25 $\mu\text{g}/\text{mL}$ of quercetin or 25 $\mu\text{g}/\text{mL}$ of TNT–Qu for 24-h cell pellet was collected and washed with PBS. Cells were fixed in 1% paraformaldehyde and stained with DNA labeling solution, incubated for 1 h at 37 °C. The cell pellet was washed with rinse buffer. The cell pellet was resuspended in propidium iodide /RNase staining buffer, incubated for 15 min in dark conditions. After completion of incubation, flow cytometry was conducted and data was analyzed by using FlowJo (BD LSRFortessa).

Immunoblotting technique

Immunoblotting was used to study the expression levels of cleaved caspase-3, an apoptotic protein. Cells were treated with 40 $\mu\text{g}/\text{mL}$ of TNT, 25 $\mu\text{g}/\text{mL}$ of quercetin or 25 $\mu\text{g}/\text{mL}$ of TNT–Qu, and cells were lysed using RIPA buffer with protease and phosphatase inhibitors. 5X SDS loading buffer

was added to the cell lysate and the lysate was denatured at 90 °C for 5 min and 50 µg of protein was loaded on each well of 12% SDS-PAGE. The gel was transferred to a nitrocellulose membrane and blocked with 5% bovine serum albumin (BSA) at room temperature. The membrane was incubated with primary antibodies against cleaved caspase-3, and actin was diluted in 5% BSA in TBST in the ratio of 1:1000 which was then kept overnight at 4 °C. The membrane was then incubated with HRP-conjugated IgG(H/L) secondary antibodies 1:3000 dilutions in 5% BSA in TBST against rabbit for 1 h at room temperature. Signal fire ECL reagent was used as a chemiluminescent substrate and analyzed using G box Chemi imaging system and protein band density was quantified using Image J software, with actin used as a loading control.

Statistical analysis

All experiments were performed at least thrice. Values were shown as mean \pm standard deviation (SD). Statistical tests were analyzed with two-way analysis of variance (ANOVA) and unpaired *T* tests using prism 8.4.1 software. Value $p < 0.05$ was considered as statistically significant.

Results and discussion

Characterization of TNT, quercetin and TNT–Qu

In this study, TNT was synthesized using the hydrothermal method and conjugated with bioflavonoid quercetin. The formed compounds TNT, TNT–Qu were characterized by XRD, FT-IR, and UV–visible spectrometry and HR-TEM analysis. XRD patterns of the TNT, quercetin and TNT–Qu are plotted in Fig. 1a. From the figure, it was clear that by the addition of quercetin, the crystallization of the TNT was slightly affected. The broadened peaks in the composite represent the blending of quercetin with the TNT at the nanoscale level. The peaks observed at 25.3°, 37.8°, 48.1°, 53.9°, 55.1°, and 62.7° correspond to (1 0 1), (0 0 4), (2 0 0), (1 0 5), (2 1 1) and (2 0 4) planes of TiO₂ standard JCPDS card number 21-1272 [24–26]. The peaks were observed at 2θ values at 27°, 12° and 10°, corresponding to Quercetin which is matched standard quercetin JCPDS card number 43-1685 [27, 28]. The XRD pattern of TNT–Qu shows peaks at 25.3, 27, 48 and 53° which reveals that the synthesized compound is in

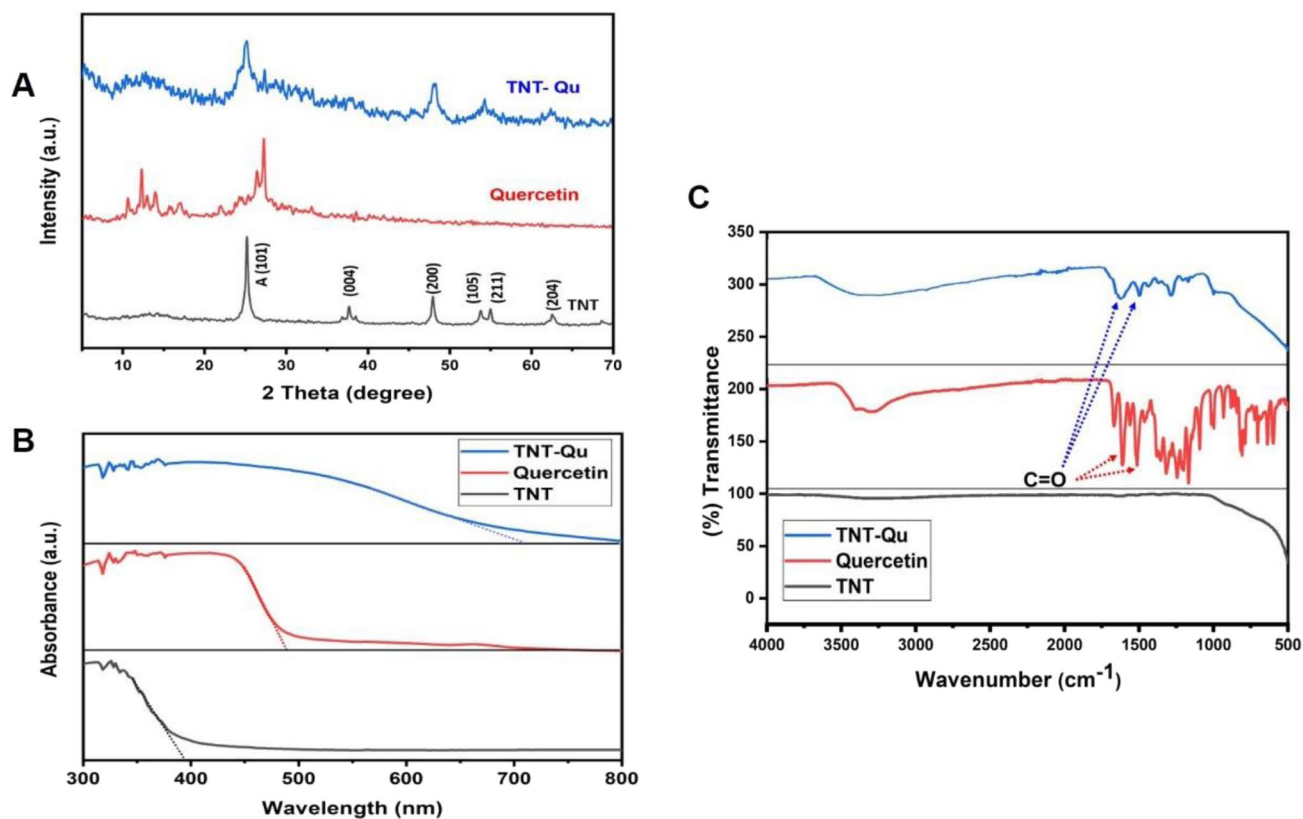


Fig. 1 Characterization of TNT, quercetin, and TNT–Qu. **a** Represents XRD pattern of TNT, quercetin and TNT–Qu. **b** DRS UV–Vis spectra of TNT, quercetin and TNT–Qu. **c** FT-IR spectra of TNT, quercetin and TNT–Qu



crystalline form and pattern correlates with the TNT and quercetin [29].

The optical properties of the TNT, quercetin, and TNT–Qu were characterized by DRS UV–Visible analysis and the results are depicted in Fig. 1b. Pristine TNT shows absorbance at 390 nm which is similar to the results of Li et al. [30]. Whereas, pure quercetin shows absorbance at 487 nm [31]. The absorbance edge of the TNT–Qu is increased and shows absorbance in visible region at a wavelength of 700 nm. This extension of the absorption edge of TNT–Qu is due to the addition of quercetin at appropriate proportion and nanoscale interface formed between TNT and quercetin.

Fourier transform infrared spectroscopy (FT-IR) was carried out on the TNT, quercetin and TNT–Qu to understand the mechanism of conjugation between TNT and quercetin. Major peaks' shift appeared from quercetin to TNT–Qu at three different wavenumbers. A peak at 1664 cm^{-1} corresponds to the C=O (Qu) converted to a higher wavelength 1690 cm^{-1} in the case of TNT–Qu with decreased intensity (Fig. 1c). This suggests the possible formation of TNT–Qu conjugates. Major peak present in quercetin at 1614 cm^{-1} shifted to 1620 cm^{-1}

in TNT–Qu also indicates the conjugation [32, 33] formed between TNT–Qu. IR peak at 1514 cm^{-1} in Qu shifted to a lower wavelength of 1497 cm^{-1} related to the Phenolic C–O stretching vibration of Qu bonded to TNT.

FT-IR peaks at 1358 and 3449 cm^{-1} correspond to Ti–O–Ti stretching and O–H stretching of TNT, respectively [34]. By adding quercetin, the additional stretching was incorporated which confirms the presence of quercetin and its conjugation to be a combination of dative, and hydrogen bonding between TNT and Qu in a composite. HR-TEM images clearly showed the prepared TNT is in tubular structure and the presence of quercetin in TNT. The average diameters of the TNT and TNT–Qu are 11.35 and 9.49 nm . The elemental components present in TNT–Qu are represented in (Fig. 2c).

Enhanced anticancer activity of TNT–Qu towards B16F10 melanoma cells

The anticancer activity of TNT, quercetin, and TNT–Qu were evaluated using B16F10 melanoma cells at 0, 10, 20,

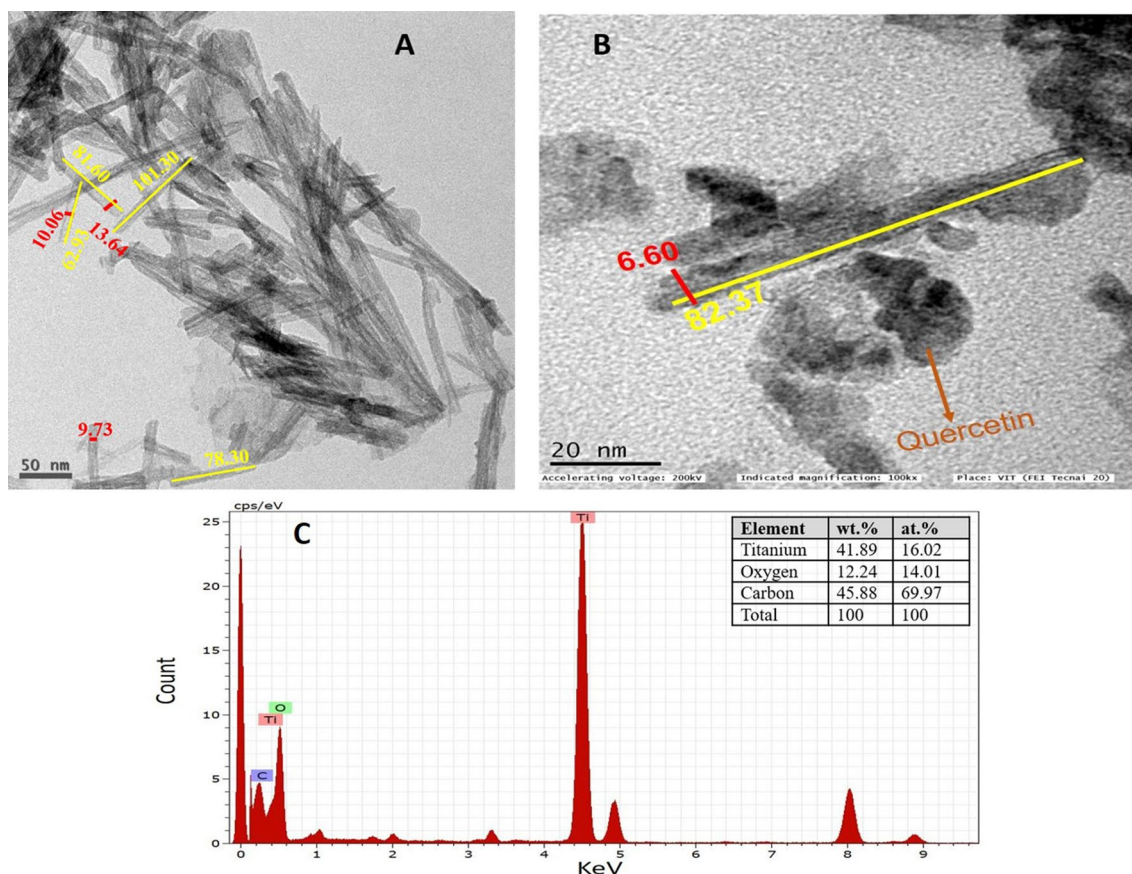


Fig. 2 Transmission electron microscope (TEM) of TNT and TNT–Qu nanostructures. **a** TNT. **b** TNT–Qu, the attachment of quercetin to TNT was represented with arrow. **c** The elemental composition of

TNT–Qu shows the presence of 41.89 wt% titanium, 12.24 wt% oxygen and 45.88 wt% carbon

40, 60, 80, 100 $\mu\text{g}/\text{mL}$ concentrations for 24 h. The cytotoxicity was measured using the MTT assay. The IC₅₀ values obtained were 72, 34 and 25 $\mu\text{g}/\text{mL}$ for TNT, quercetin and

TNT–Qu treatment, respectively indicating that TNT–Qu exhibited better cytotoxicity when compared to quercetin or TNT alone treatment in a dose-dependent manner (Fig. 3).

Fig. 3 Cytotoxic effect of TNT, quercetin, and TNT–Qu on B16F10 melanoma cells assessed by MTT assay. Survival of B16F10 cells after 24 h exposure to TNT, quercetin and TNT–Qu at 0–100 $\mu\text{g}/\text{mL}$ concentration. Cell cytotoxicity was measured by the MTT assay. Data are represented as mean \pm SD

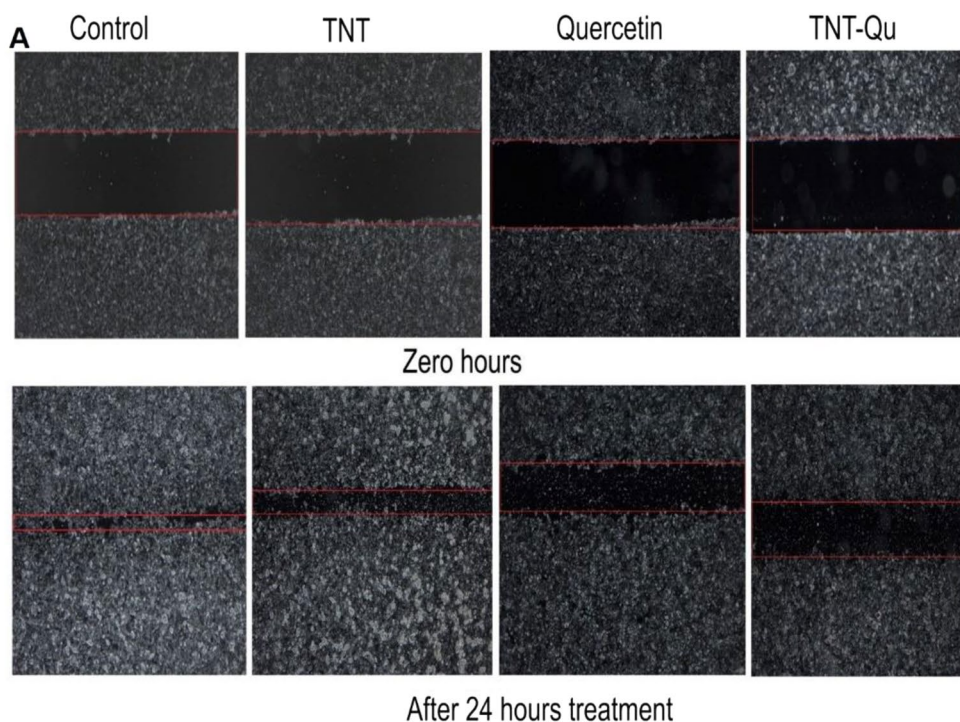
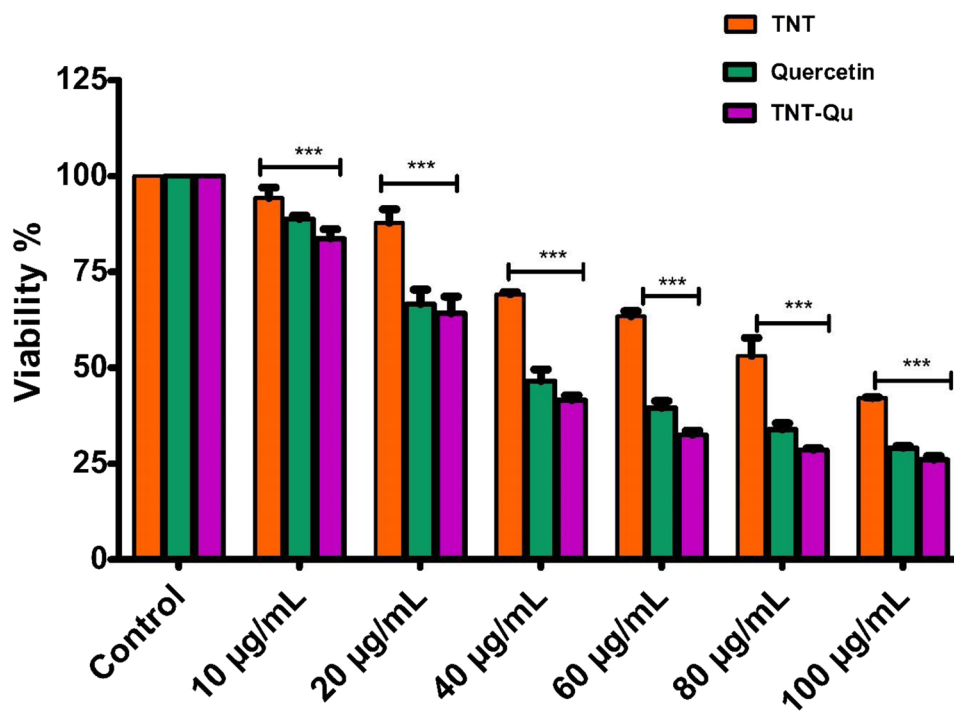


Fig. 4 TNT–Qu suppresses the migration of B16F10 cells. **a** Migration analysis of B16F10 cells treated with TNT, quercetin and TNT–Qu for 24 h. TNT–Qu highly inhibited the migration of cells. Cell migration was assessed by wound healing assay and compared to the

cells with no treatment. **b** Graphical representation of scratch width before and after treatment with TNT, quercetin and TNT–Qu $N=3$. Data are presented as mean \pm SD

These results demonstrate the effectiveness of TNT–Qu as a potent anticancer agent. Our previous studies have shown that TNT was cytotoxic to the MDA-MB231 cancer cell line and there was no significant difference in the survival of normal 3T3 fibroblast cells [11]. Also, quercetin was shown to be non-toxic to normal cell lines [35].

Pradhan et al. [36] showed that quercetin was efficient in inhibiting migration and proliferation of B16F10 cells at 50 μM concentration. Quercetin also acts as an emerging anti-melanoma agent by enhancing p53 and Nrf2 levels [37, 38]. Quercetin conjugated to different nanoparticles inhibited proliferation of various cancer cell lines than quercetin alone; silver, superparamagnetic and gold nanoparticles conjugated with quercetin inhibited growth of human breast cancer cell lines than quercetin alone and a varying range of IC50 values were reported [23, 39, 40]. Although earlier reports showed that TNT and quercetin individually exhibited anticancer activity, this study is the first to show the enhanced anticancer activity of TNT–Qu. Hence, TNT–Qu could be a potential combinational anticancer agent for the treatment of skin cancer.

Inhibition effect of TNT–Qu on the migration of B16F10

Migration of cells is enhanced in tumor microenvironment and metastasis. The migration effect of the TNT, quercetin and TNT–Qu was studied using the scratch assay and the results are depicted in Fig. 4. First scratch was created as described in methods and then cells were treated with TNT 40 $\mu\text{g}/\text{mL}$, quercetin 25 $\mu\text{g}/\text{mL}$ or TNT–Qu with 25 $\mu\text{g}/\text{mL}$. After 24 h of treatment, we found that TNT–Qu significantly inhibited the migration of the melanoma cells more than quercetin or TNT alone. These data indicate that TNT–Qu had more anticancer activity when compared to quercetin and TNT alone. The quantity of migration was analyzed by recording the pictures at 0 and 24 h, while the movement of migration was analyzed using Image J software [41]. These data agree with the previous studies showing that quercetin inhibited the migration of numerous cancer cell lines [42–44]. Also, Cao et al. [17] reported that quercetin inhibited the migration of B16F10.

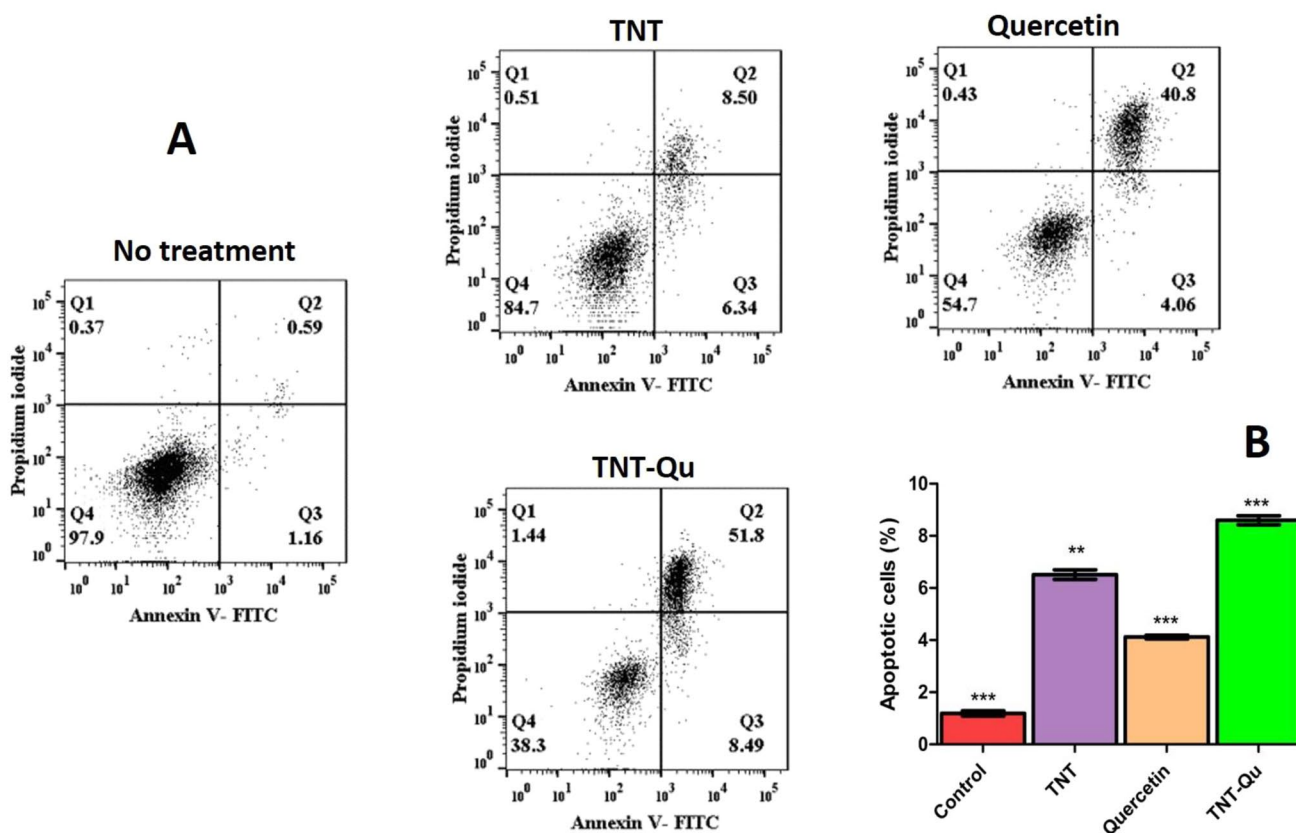


Fig. 5 TNT–Qu accelerates the apoptosis in B16F10. **a** Induction of the apoptosis in B16F10 cells after 24 h of treatment with TNT 40 $\mu\text{g}/\text{mL}$, quercetin and TNT–Qu at 25 $\mu\text{g}/\text{mL}$ concentration was assessed flow cytometry annexin V/PI. The histograms show the live,

early apoptosis, apoptosis and necrotic cells percentage. Early and late apoptotic and necrotic levels are more in TNT–Qu treatment. **b** Total apoptosis percentage is represented graphically. Error bars indicate as mean \pm SD

TNT, quercetin and TNT–Qu induced apoptosis

In the early events of apoptosis, translocation of membrane phosphatidylserine from the inner plasma membrane to surface of the plasma membrane occurs. Annexin V has a great affinity towards phosphatidylserine [45]. To study the apoptotic effect of TNT, quercetin and TNT–Qu on B16F10, cells were treated and incubated with Annexin V–FITC and PI. The percentage of early and late apoptotic cells in untreated control, TNT-, quercetin- and TNT–Qu-treated B16F10 cells was 1.75, 14.84, 44.86 and 60.29%, respectively, as shown in Fig. 5. Early and late apoptotic and necrotic cells were high in TNT–Qu-treated B16F10 cells when compared to quercetin- and TNT-alone-treated cells. Apoptosis plays an important role in the pathogenesis of many diseases. In cancer cells, the level of apoptosis is too low, and the mechanism is complex which involves different pathways [46]. Quercetin has been shown to induce apoptosis in liver cancer cells, breast cancer, human prostate PC3, acute ovarian cancer

cells at concentrations ranging from 20 to 120 μM [47, 48], and also quercetin promotes apoptosis in UV-B-irradiated B16F10 melanoma cells [49].

Quercetin and TNT–Qu reduces ROS generation

The requirement of ROS in cancer cells is higher than normal cells; if the content of ROS lower than the minimum requirement of cellular response, cancer cells will not grow [50–52]. To investigate the ability of TNT, quercetin and TNT–Qu to generate ROS on B16F10 cells, cellular ROS/superoxide kit was used which contains fluorescent dye DCFH-DA and superoxide's detection reagent. DCF and superoxide's fluorescence was measured using flow cytometry. Pyocyanin used as a positive control induces both superoxides and ROS; *N*-acetyl-L cysteine is used as a negative control. Cells treated with quercetin and TNT–Qu reduced ROS and superoxides than control ones due to its antioxidant property, while TNT alone treatment does not show any

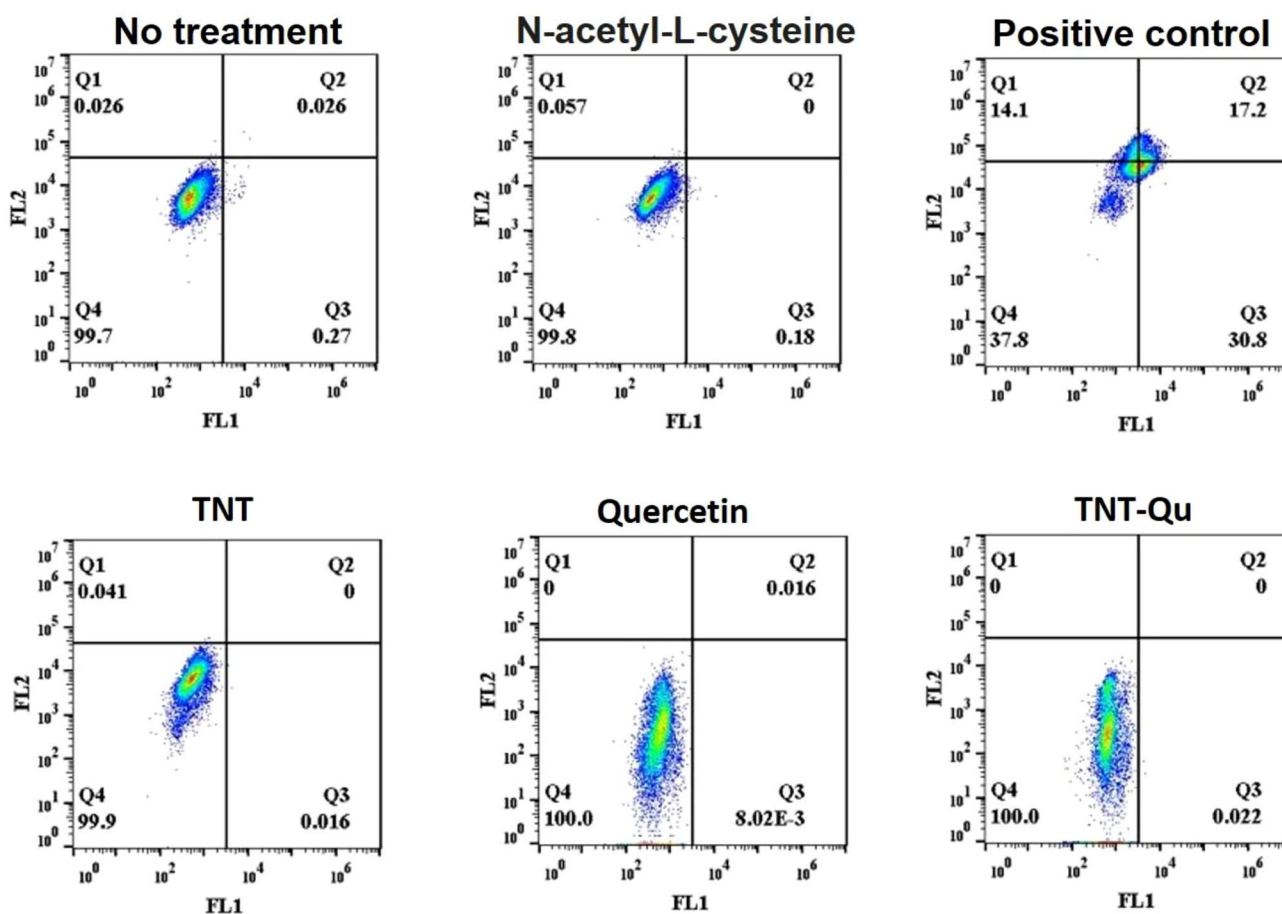


Fig. 6 Quercetin and TNT–Qu down-regulates ROS and superoxides. Effect of TNT, quercetin and TNT–Qu on ROS and superoxide levels were measured by treating B16F10 cells with TNT, quercetin and TNT–Qu for 24 h. 100 μM pyocyanin is used as a positive control and

N-acetyl-cysteine as a negative control, untreated cells were used as no treatment. The results shown are representative of three experiments



effect (Fig. 6). Due to the antioxidant property of quercetin, it does not enhance the ROS levels [53]. To support this, Rather a Rafiq et al. also demonstrated that quercetin alone effectively decreases ROS levels in B16F10 cells. Also Shikha Srivastava et al. demonstrated that in leukemic cell line quercetin interacts with DNA, arrested cell cycle and promoted apoptosis. However, it does not induce ROS levels, suggesting that quercetin may act as an antioxidant [49, 54].

TNT, quercetin and TNT–Qu enhanced DNA fragmentation

A later step in apoptosis is the cleavage of chromosomal DNA into oligonucleotide fragments. To study the ability of TNT, quercetin, and TNT–Qu on DNA fragmentation, a TUNEL assay was performed. Cells treated with TNT–Qu induced more DNA fragments than quercetin or TNT alone (Fig. 7). Histogram analysis represented the DNA nick labelled population of 2.46% for TNT showed, 18.7% for quercetin, and 20.6% for TNT–Qu. This data further confirms that TNT–Qu induced more DNA fragments than TNT

or quercetin alone. These results revealed that B16F10 cells treated with these compounds induced more DNA fragments when compared to control cells (no treatment). These data support that TNT, quercetin and TNT–Qu induce apoptosis. Our results revealed that TNT–Qu treatment breaks DNA into oligonucleotide fragments more than quercetin or TNT alone and these data co-relate with apoptosis data.

TNT–Qu treatment arrested cell cycle at G2/M

One of the key hallmarks of apoptosis is cell cycle regulation. Cell cycle analysis was done using DAPI. After completion of the treatment, cells were stained with DAPI and analyzed by flow cytometry. B16F10 cells treated with TNT, quercetin, and TNT–Qu arrested the cell cycle at the G2/M phase. The percent positive cells as shown in Fig. 8 arrested in G2/M were high in TNT–Qu treated 50.5%, compared to TNT 3.71% and quercetin alone 30%. Cells treated with TNT enhance the cell number (23%) at sub G1 phase. These results demonstrated that G2/M cell arrest is due to the permanent DNA damage on cells

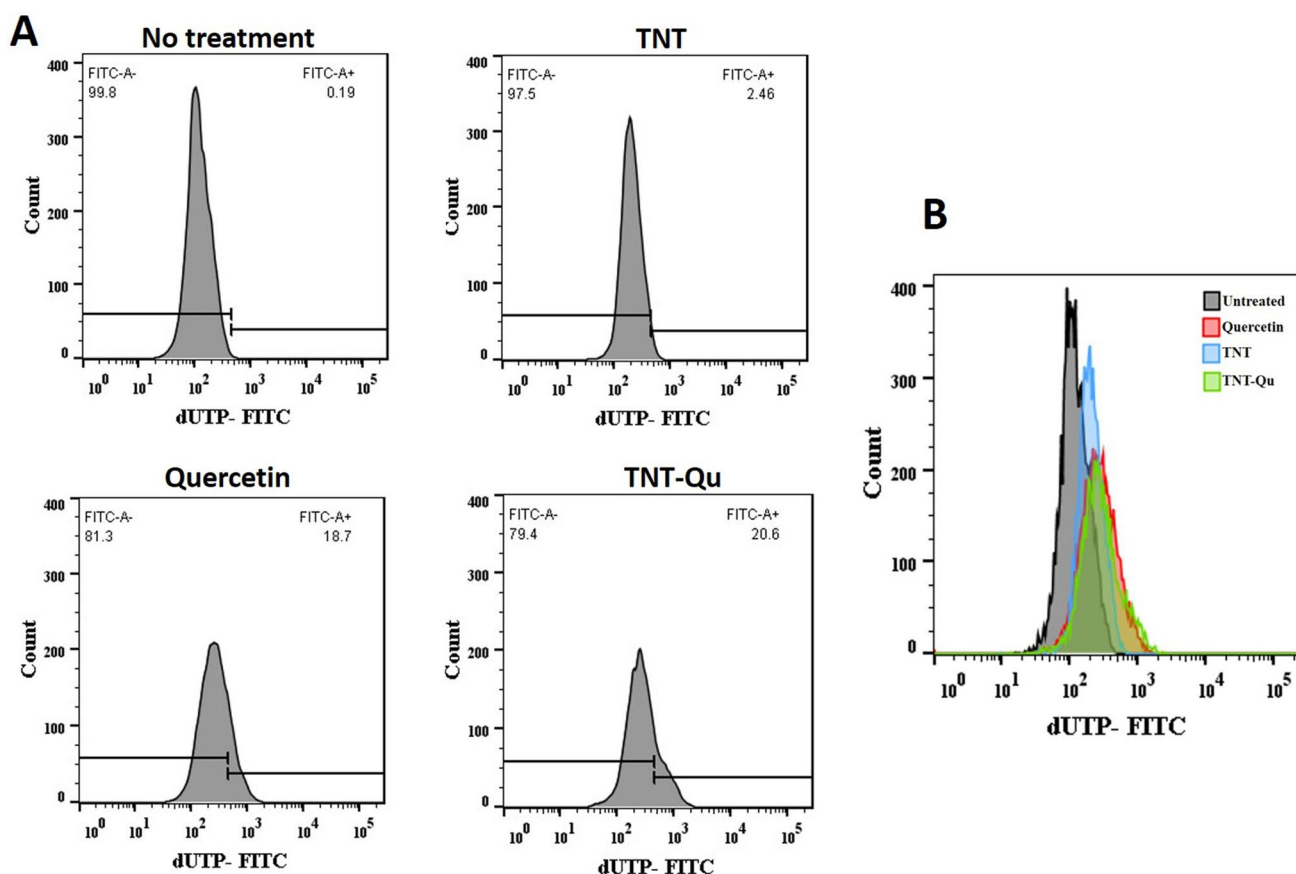


Fig. 7 TNT–Qu treatment enhances DNA fragments. **a** TUNEL assay was used to estimate the percentage of DNA fragments of B16F10 cells exposed to TNT, quercetin or TNT–Qu for 24 h. The histograms

show the percentage of DNA fragments. **b** comparative representation of DNA fragments of B16F10 cells treated with TNT, quercetin or TNT–Qu. The results shown are representative of three experiments



and consistent with above apoptosis and DNA fragmentation data. These results support that TNT–Qu had a higher influence in arresting the cell cycle number at the G2/M phase. Several studies suggested that permanent DNA damage induces cell cycle arrest G2/M phase and also overexpression of P53 leads to G2/M arrest [55, 56]. Choi et al. also reported that quercetin arrested the cell cycle at G2/M phase in breast carcinoma, adenocarcinoma, and leukemia cell lines [54, 57, 58]. Collectively, these data revealed that DNA fragmentation had a high chance of developing apoptosis. The observed cell cycle arrest at G2/M phase was also consistent with the permanent DNA damage within the cells.

TNT–Qu up-regulated apoptotic protein cleaved caspase-3

Further, to understand the molecular mechanism of quercetin, TNT, TNT–Qu on B16F10, immunoblotting was performed for caspase-3. In apoptosis, caspases are key mediators. Among the caspases, caspase-3 is crucial for DNA fragmentation and apoptotic chromatin condensation and highly regulated in cancer cells [59, 60]. Hence, this study focused on the expression of cleaved caspase-3 by western blot after cells were treated with TNT, quercetin and TNT–Qu. Cleaved caspase-3 was detected in all treatments (Fig. 9). Our results revealed

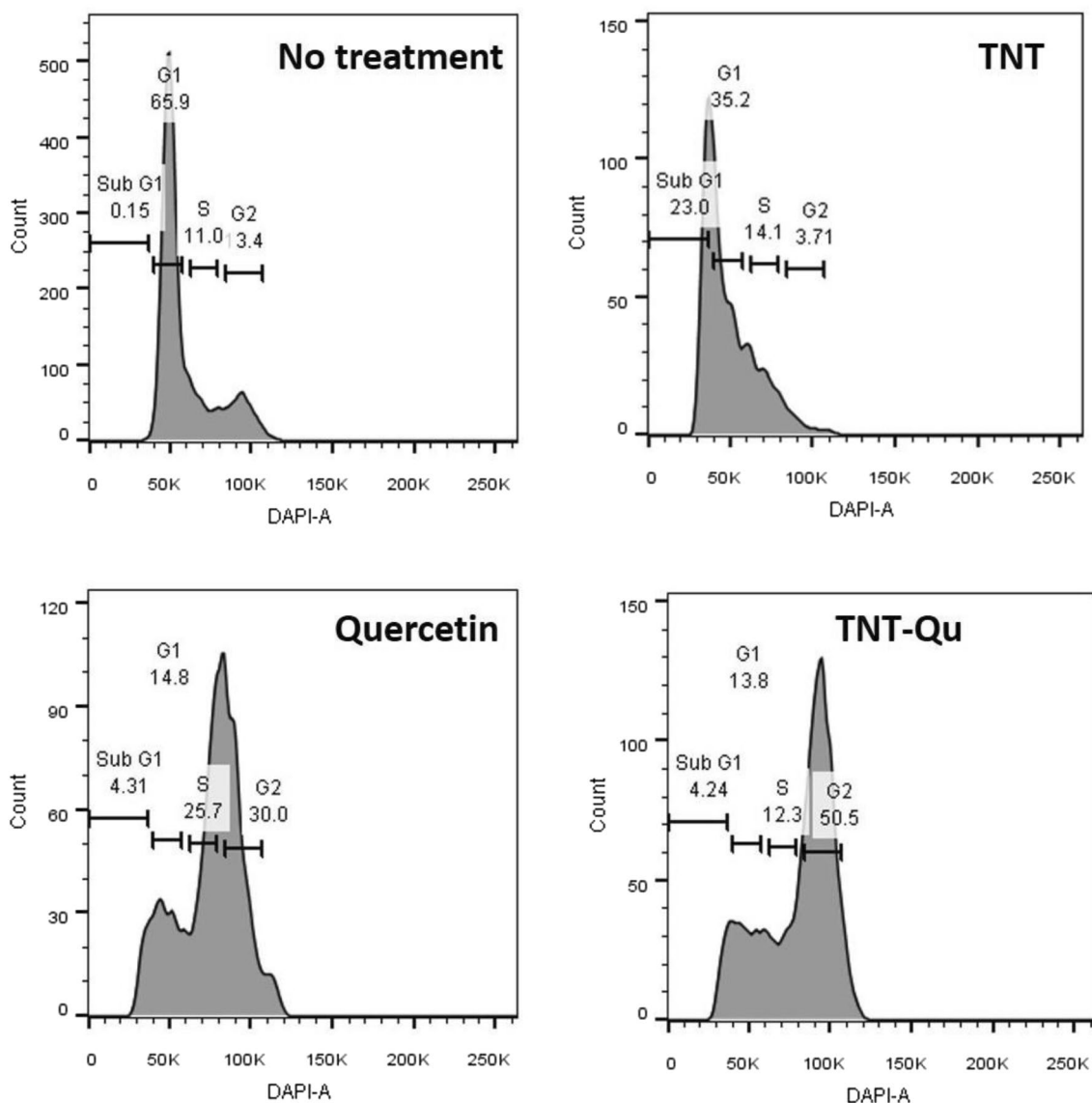


Fig. 8 TNT–Qu promotes cell cycle arrest at G2/M. Effect of the TNT, Quercetin and TNT–Qu on regulation of cell cycle in B16F10 cells. The histograms represent the distribution of the cells at sub G1,

G1, S and G2/M phase. After completion of the treatment, cells were stained with DAPI and cell cycle regulation was analyzed using flow cytometry. The results were represented by three independent assays



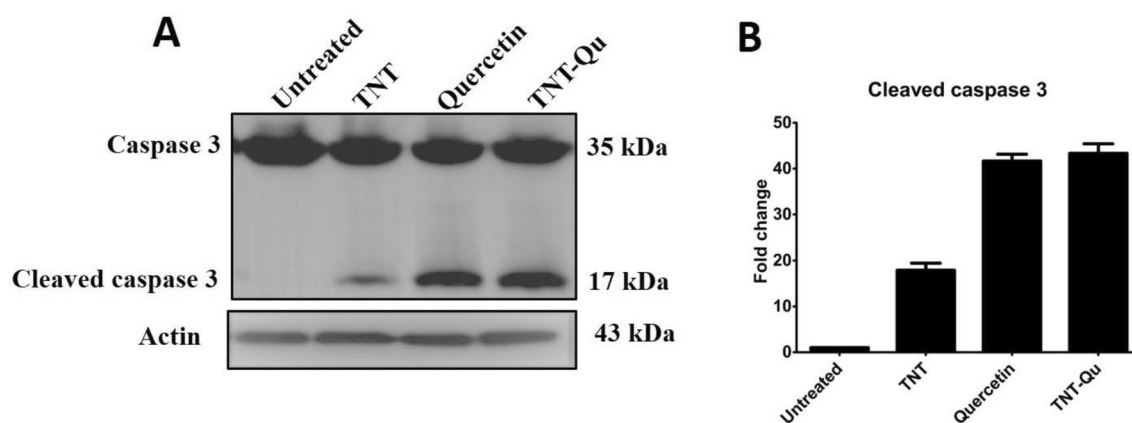


Fig. 9 TNT–Qu treatment up-regulated the apoptotic marker. **a** Expression of cleaved caspase-3 protein levels following 24-h treatment of TNT, quercetin or TNT–Qu by western blotting. **b** Increased

fold change in the expression of cleaved caspase-3 upon TNT, quercetin and TNT–Qu treatment after normalization of western blot data. Data are presented as mean \pm SD

that TNT–Qu treatment up-regulated the expression of cleaved caspase-3 in B16F10 and this data is consistent with Annexin V–FITC staining data (Fig. 5). All these results support that TNT–Qu, quercetin and TNT induce apoptosis in B16F10 cells. Our data demonstrated that TNT–Qu treatment enhanced the cleaved caspase-3 expression when compared to TNT, quercetin alone. Earlier studies described that quercetin enhanced apoptosis by caspase-3 in various cell lines MDA-MB-231, HL-60 [61, 62].

Conclusion

Cancer is the leading cause of death globally and finding a non-toxic, efficient drug for the treatment of cancer is urgently needed. Combination therapy is gaining attention from researchers worldwide. Synthesized TNT–Qu was characterized using several physicochemical methods. The cytotoxicity results revealed that TNT–Qu is more cytotoxic than TNT, quercetin alone. Furthermore, inhibition effect of TNT–Qu on the migration of B16F10 melanoma cells was observed. Mechanism of anticancer activity of TNT, quercetin and TNT–Qu was analyzed and found that TNT–Qu induced apoptosis in B16F10 cells and enhanced the DNA fragments, arrested cell cycle at G2/M phase. Moreover, TNT–Qu, quercetin, and TNT enhanced the cleavage of caspase-3 expression in B16F10 cells. All of these results revealed that TNT–Qu is a potent anticancer agent when compared to quercetin alone or TNT alone. Hence, these studies would be helpful for studying the in vivo models and clinical use of TNT–Qu as a potential therapeutic combinational molecule for the treatment of cancer.

Acknowledgements Taif University researchers supporting project number (TURSP-2020/04), Taif University, Taif, Saudi Arabia.

Author contributions SG, MC, DL, AS, and MKM conceived the experiment, SG performed the experiments, PBA, MCR interpreted the results. SG, DL, KRR, I and TAT wrote the first version and all authors contributed in improving the manuscript until reaching the final version.

Declarations

Conflict of interest The authors declare no conflict of interests.

References

- Garrubba, C., Donkers, K.: Skin cancer. *JAAPA* **33**, 49–50 (2020)
- Cichorek, M., Wachulska, M., Stasiewicz, A., Tymińska, A.: Skin melanocytes: biology and development. *Postep. Dermatol. Alergol.* **30**, 30 (2013)
- Nataraj, A.J., Trent, J.C., 2nd., Ananthaswamy, H.N.: p53 gene mutations and photocarcinogenesis. *Photochem. Photobiol.* **62**, 218–230 (1995)
- Soehnge, H., Ouhtit, A., Ananthaswamy, O.N.: Mechanisms of induction of skin cancer by UV radiation. *Front. Biosci.* **2**, d538–551 (1997)
- Howard, M.D., Xie, C., Wee, E., Wolfe, R., McLean, C.A., Kelly, J.W., Pan, Y.: Acral lentiginous melanoma: differences in survival compared with other subtypes. *Br. J. Dermatol.* **182**, 1056–1057 (2020)
- Barnhill, R.L.: Malignant melanoma. In: Klaus J. (Eds.) *Pathology of melanocytic nevi and malignant melanoma*. pp. 238–356. Springer, (2004).
- Gullaa, S., Lomadab, D., Srikanthc, V.V., Shankard, M.V., Reddy, K.R., Sonif, S., Reddy, M.C.: Recent advances in nanoparticles-based strategies for cancer therapeutics and antibacterial applications. *Nanotechnology* **46**, 255–293 (2019)
- Subbiah, R., Veerapandian, M., Yun, K.S.: Nanoparticles: functionalization and multifunctional applications in biomedical sciences. *Curr. Med. Chem.* **17**, 4559–4577 (2010)

9. Ashree, J., Wang, Q., Chao, Y.: Glyco-functionalised quantum dots and their progress in cancer diagnosis and treatment. *Front. Chem. Sci. Eng.* **14**, 1–13 (2019)
10. Zhou, W., Liu, H., Boughton, R.I., Du, G., Lin, J., Wang, J., Liu, D.: One-dimensional single-crystalline Ti–O based nanostructures: properties, synthesis, modifications and applications. *J. Mater. Chem.* **20**, 5993–6008 (2010)
11. Latha, T.S., Reddy, M.C., Muthukonda, S.V., Srikanth, V.V., Lomada, D.: In vitro and in vivo evaluation of anti-cancer activity: shape-dependent properties of TiO₂ nanostructures. *Mater. Sci. Eng. C* **78**, 969–977 (2017)
12. Latha, T.S., Reddy, M.C., Durbaka, P.V., Muthukonda, S.V., Lomada, D.: Immunomodulatory properties of titanium dioxide nanostructural materials. *Indian J. Pharmacol.* **49**, 458 (2017)
13. Hu, C.M.J., Zhang, L.: Therapeutic nanoparticles to combat cancer drug resistance. *Curr. Drug Metabol.* **10**, 836–841 (2009)
14. Dadwal, A., Baldi, A., Kumar Narang, R.: Nanoparticles as carriers for drug delivery in cancer. *Artif. Cell Blood Substit. Biotechnol.* **46**, 295–305 (2018)
15. Zhang, J., Tang, H., Liu, Z., Chen, B.: Effects of major parameters of nanoparticles on their physical and chemical properties and recent application of nanodrug delivery system in targeted chemotherapy. *Int. J. Nanomed.* **12**, 8483 (2017)
16. Umot, E.: Surface modification of nanoparticles used in biomedical applications. *Mod. Surf. Eng. Treat.* **20**, 185–208 (2013)
17. Cao, H.H., Tse, A.K., Kwan, H.Y., Yu, H., Cheng, C.Y., Su, T., Fong, W.F., Yu, Z.L.: Quercetin exerts anti-melanoma activities and inhibits STAT3 signaling. *Biochem. Pharmacol.* **87**, 424–434 (2014)
18. Spagnuolo, C., Russo, M., Bilotto, S., Tedesco, I., Laratta, B., Russo, G.L.: Dietary polyphenols in cancer prevention: the example of the flavonoid quercetin in leukemia. *Ann. N. Y. Acad. Sci.* **1259**, 95–103 (2012)
19. Sezer, E.D., Oktay, L.M., Karadadaş, E., Memmedov, H., Selvi Gunel, N., Sözmen, E.: Assessing anticancer potential of blueberry flavonoids, quercetin, kaempferol, and genticic acid, through oxidative stress and apoptosis parameters on HCT-116 cells. *J. Med. Food* **22**, 1118–1126 (2019)
20. Michaud-Levesque, J., Bousquet-Gagnon, N., Béliveau, R.: Quercetin abrogates IL-6/STAT3 signaling and inhibits glioblastoma cell line growth and migration. *Exp. Cell Res.* **318**, 925–935 (2012)
21. Kim, Y.J.: Hyperin and quercetin modulate oxidative stress-induced melanogenesis. *Biol. Pharm. Bull.* **35**, 2023–2027 (2012)
22. Kumar, D.P., Reddy, N.L., Kumari, M.M., Srinivas, B., Kumari, V.D., Sreedhar, B., Roddatis, V., Bondarchuk, O., Karthik, M., Neppolian, B.: Cu₂O-sensitized TiO₂ nanorods with nanocavities for highly efficient photocatalytic hydrogen production under solar irradiation. *Sol. Energy Mater. Sol. Cells* **136**, 157–166 (2015)
23. Balakrishnan, S., Mukherjee, S., Das, S., Bhat, F.A., Raja Singh, P., Patra, C.R., Arunakaran, J.: Gold nanoparticles-conjugated quercetin induces apoptosis via inhibition of EGFR/PI3K/Akt-mediated pathway in breast cancer cell lines (MCF-7 and MDA-MB-231). *Cell. Biochem. Funct.* **35**, 217–231 (2017)
24. Kumar, D.P., Reddy, N.L., Karthik, M., Neppolian, B., Madhavan, J., Shankar, M.: Solar light sensitized p-Ag₂O/n-TiO₂ nanotubes heterojunction photocatalysts for enhanced hydrogen production in aqueous-glycerol solution. *Sol. Energy Mater. Sol. Cells* **154**, 78–87 (2016)
25. Kumari, M.M., Priyanka, A., Mareenna, B., Haridoss, P., Kumar, D.P., Shankar, M.: Benefits of tubular morphologies on electron transfer properties in CNT/TiNT nanohybrid photocatalyst for enhanced H₂ production. *RSC Adv.* **7**, 7203–7209 (2017)
26. MamathaKumari, M., Kumar, D.P., Haridoss, P., Durgakumari, V., Shankar, M.: Nanohybrid of titania/carbon nanotubes–nanohorns: a promising photocatalyst for enhanced hydrogen production under solar irradiation. *Int. J. Hydrog. Energy* **40**, 1665–1674 (2015)
27. Yadav, S., Mehrotra, G.K., Bhartiya, P., Singh, A., Dutta, P.K.: Preparation, physicochemical and biological evaluation of quercetin based chitosan-gelatin film for food packaging. *Carbohydr. Polym.* **227**, 115348 (2020)
28. Borghetti, G., Carini, J., Honorato, S., Ayala, A., Moreira, J., Bassani, V.: Physicochemical properties and thermal stability of quercetin hydrates in the solid state. *Thermochim. Acta* **539**, 109–114 (2012)
29. Amanzadeh, E., Esmaeili, A., Abadi, R.E.N., Kazemipour, N., Pahlevanneshan, Z., Beheshti, S.: Quercetin conjugated with superparamagnetic iron oxide nanoparticles improves learning and memory better than free quercetin via interacting with proteins involved in LTP. *Sci. Rep.* **9**, 1–19 (2019)
30. Li, C., Zong, L., Li, Q., Zhang, J., Yang, J., Jin, Z.: Photocatalytic oxidation of propylene on Pd-loaded anatase TiO₂ nanotubes under visible light irradiation. *Nanoscale Res Lett.* **11**, 1–8 (2016)
31. Amorati, R., Baschieri, A., Cowden, A., Valgimigli, L.: The anti-oxidant activity of quercetin in water solution. *Biomimetics* **2**, 1–13 (2017)
32. Bellamy, L.: *The infra-red spectra of complex molecules*. Springer, Dordrecht (2013)
33. Sri, K.V., Kondaiah, A., Ratna, J.V., Annapurna, A.: Preparation and characterization of quercetin and rutin cyclodextrin inclusion complexes. *Drug Dev. Ind. Pharm.* **33**, 245–253 (2007)
34. Madhusudhan, A., Reddy, G.B., Venkatesham, M., Veerabhadram, G., Kumar, D.A., Natarajan, S., Yang, M.Y., Hu, A., Singh, S.S.: Efficient pH dependent drug delivery to target cancer cells by gold nanoparticles capped with carboxymethyl chitosan. *Int. J. Mol. Sci.* **15**, 8216–8234 (2014)
35. Son, Y.-O., Lee, K.-Y., Kook, S.-H., Lee, J.-C., Kim, J.-G., Jeon, Y.-M., Jang, Y.-S.: Selective effects of quercetin on the cell growth and anti-oxidant defense system in normal versus transformed mouse hepatic cell lines. *Eur. J. Pharmacol.* **502**, 195–204 (2004)
36. Pradhan, S.J., Mishra, R., Sharma, P., Kundu, G.C.: Quercetin and sulfuraphane in combination suppress the progression of melanoma through the down-regulation of matrix metalloproteinase-9. *Exp. Ther. Med.* **1**, 915–920 (2010)
37. Harris, Z., Donovan, M.G., Branco, G.M., Limesand, K.H., Burd, R.: Quercetin as an emerging anti-melanoma agent: a four-focus area therapeutic development strategy. *Front. Nutr.* **3**, 48 (2016)
38. Nasr, M., Al-Karaki, R.: Nanotechnological innovations enhancing the topical therapeutic efficacy of quercetin: a succinct review. *Curr. Drug Deliv.* **17**, 270–278 (2020)
39. Aghapour, F., Moghadamnia, A.A., Nicolini, A., Kani, S.N.M., Barari, L., Morakabati, P., Rezazadeh, L., Kazemi, S.: Quercetin conjugated with silica nanoparticles inhibits tumor growth in MCF-7 breast cancer cell lines. *Biochem. Biophys. Res. Commun.* **500**, 860–865 (2018)
40. Kumar, S.R., Priyatharshni, S., Babu, V.N., Mangalaraj, D., Viswanathan, C., Kannan, S., Ponpandian, N.: Quercetin conjugated superparamagnetic magnetite nanoparticles for in-vitro analysis of breast cancer cell lines for chemotherapy applications. *J. Colloid Interface Sci.* **436**, 234–242 (2014)
41. Liang, C.C., Park, A.Y., Guan, J.L.: In vitro scratch assay: a convenient and inexpensive method for analysis of cell migration in vitro. *Nat. Protoc.* **2**, 329–333 (2007)
42. Kim, S.R., Lee, E.Y., Kim, D.J., Kim, H.J., Park, H.R.: Quercetin inhibits cell survival and metastatic ability via the EMT-mediated pathway in oral squamous cell carcinoma. *Molecules* **25**, 757 (2020)
43. Dong, Y., Yang, J., Yang, L., Li, P.: Quercetin inhibits the proliferation and metastasis of human non-small cell lung cancer cell line: the key role of Src-mediated fibroblast growth factor-inducible 14



- (Fn14)/nuclear factor kappa B (NF- κ B) pathway. *Med. Sci. Monit.* **26**, e920537-1-e920537-11 (2020)
44. Vafadar, A., Shabaninejad, Z., Movahedpour, A., Fallahi, F., Taghavi, M., Ghasemi, Y., Akbari, M., Shafiee, A., Hajighadimi, S., Moradzarmehri, S.: Quercetin and cancer: new insights into its therapeutic effects on ovarian cancer cells. *Cell Biosci.* **10**, 1–17 (2020)
 45. Demchenko, A.P.: Beyond annexin V: fluorescence response of cellular membranes to apoptosis. *Cytotechnology* **65**, 157–172 (2013)
 46. Warren, C.F.A., Wong-Brown, M.W., Bowden, N.A.: BCL-2 family isoforms in apoptosis and cancer. *Cell Death Dis.* **10**, 177 (2019)
 47. Hashemzaei, M., Delarami Far, A., Yari, A., Heravi, R.E., Tabrizian, K., Taghdisi, S.M., Sadegh, S.E., Tsarouhas, K., Kouretas, D., Tzanakakis, G., Nikitovic, D., Anisimov, N.Y., Spandidos, D.A., Tsatsakis, A.M., Rezaee, R.: Anticancer and apoptosis-inducing effects of quercetin in vitro and in vivo. *Oncol. Rep.* **38**, 819–828 (2017)
 48. Srivastava, N.S., Srivastava, R.A.K.: Curcumin and quercetin synergistically inhibit cancer cell proliferation in multiple cancer cells and modulate Wnt/ β -catenin signaling and apoptotic pathways in A375 cells. *Phytomedicine* **52**, 117–128 (2019)
 49. Rafiq, R.A., Quadri, A., Nazir, L.A., Peerzada, K., Ganai, B.A., Tasduq, S.A.: A Potent inhibitor of phosphoinositide 3-kinase (PI3K) and mitogen activated protein (MAP) kinase signalling, quercetin (3, 3', 4', 5, 7-pentahydroxyflavone) promotes cell death in ultraviolet (UV)-B-irradiated B16F10 melanoma cells. *PLoS ONE* **10**, e0131253 (2015)
 50. Trachootham, D., Alexandre, J., Huang, P.: Targeting cancer cells by ROS-mediated mechanisms: a radical therapeutic approach? *Nat. Rev. Drug Discov.* **8**, 579–591 (2009)
 51. Jeong, C.H., Joo, S.H.: Downregulation of reactive oxygen species in apoptosis. *J. Cancer Prev.* **21**, 13–20 (2016)
 52. Circu, M.L., Aw, T.Y.: Reactive oxygen species, cellular redox systems, and apoptosis. *Free Radic. Biol. Med.* **48**, 749–762 (2010)
 53. Xu, D., Hu, M.J., Wang, Y.Q., Cui, Y.L.: Antioxidant activities of quercetin and its complexes for medicinal application. *Molecules* **24**, 1123 (2019)
 54. Srivastava, S., Somasagara, R.R., Hegde, M., Nishana, M., Tadi, S.K., Srivastava, M., Choudhary, B., Raghavan, S.C.: Quercetin, a natural flavonoid interacts with DNA, arrests cell cycle and causes tumor regression by activating mitochondrial pathway of apoptosis. *Sci. Rep.* **6**, 24049 (2016)
 55. Taylor, W.R., DePrimo, S.E., Agarwal, A., Agarwal, M.L., Schonthal, A.H., Katula, K.S., Stark, G.R.: Mechanisms of G2 arrest in response to overexpression of p53. *Mol. Biol. Cell* **10**, 3607–3622 (1999)
 56. Gire, V., Dulic, V.: Senescence from G2 arrest, revisited. *Cell Cycle* **14**, 297–304 (2015)
 57. Choi, J.A., Kim, J.Y., Lee, J.Y., Kang, C.M., Kwon, H.J., Yoo, Y.D., Kim, T.W., Lee, Y.S., Lee, S.J.: Induction of cell cycle arrest and apoptosis in human breast cancer cells by quercetin. *Int. J. Oncol.* **19**, 837–844 (2001)
 58. Lee, T.J., Kim, O.H., Kim, Y.H., Lim, J.H., Kim, S., Park, J.W., Kwon, T.K.: Quercetin arrests G2/M phase and induces caspase-dependent cell death in U937 cells. *Cancer Lett.* **240**, 234–242 (2006)
 59. Yu, J., Li, S., Qi, J., Chen, Z., Wu, Y., Guo, J., Wang, K., Sun, X., Zheng, J.: Cleavage of GSDME by caspase-3 determines lobaplatin-induced pyroptosis in colon cancer cells. *Cell Death Dis.* **10**, 193 (2019)
 60. Porter, A.G., Janicke, R.U.: Emerging roles of caspase-3 in apoptosis. *Cell Death Differ.* **6**, 99–104 (1999)
 61. Chien, S.Y., Wu, Y.C., Chung, J.G., Yang, J.S., Lu, H.F., Tsou, M.F., Wood, W.G., Kuo, S.J., Chen, D.R.: Quercetin-induced apoptosis acts through mitochondrial- and caspase-3-dependent pathways in human breast cancer MDA-MB-231 cells. *Hum. Exp. Toxicol.* **28**, 493–503 (2009)
 62. Niu, G., Yin, S., Xie, S., Li, Y., Nie, D., Ma, L., Wang, X., Wu, Y.: Quercetin induces apoptosis by activating caspase-3 and regulating Bcl-2 and cyclooxygenase-2 pathways in human HL-60 cells. *Acta Biochim. Biophys. Sin. (Shanghai)* **43**, 30–37 (2011)
- Publisher's Note** Springer Nature remains neutral with regard to jurisdictional claims in published maps and institutional affiliations.

